Jurnal
Teknologi

Full Paper

PRISTINE AND GROUP IV DOPED BORON NITRIDE SINGLE-WALL NANOTUBES FOR HYDROGEN STORAGE: A DENSITY FUNCTIONAL THEORY COMPUTATIONAL INVESTIGATION

Article history
Received
25 May 2022
Received in revised form
23 August 2022
Accepted
3 September 2022
Published Online
23 October 2022

Pek-Lan Toh*, Syed Amir Abbas Shah Naqvi, Suh-Miin Wang, Yao-Cong Lim

Faculty of Engineering and Green Technology, Universiti Tunku Abdul Rahman, 31900 Kampar, Perak, Malaysia

*Corresponding author
tohpl@utar.edu.my

Graphical abstract

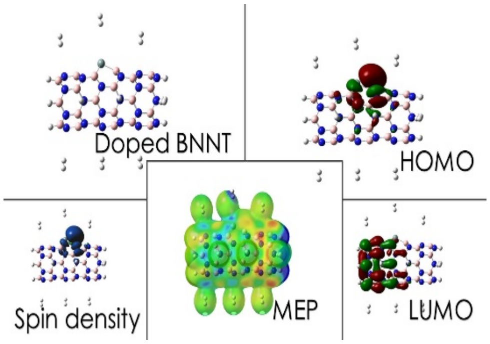

Abstract

In this report, a density functional theory (DFT) computational approach was used to investigate the structural and electronic properties of molecular hydrogens adsorbed on single-walled boron nitride nanotubes (BNNTs) with/without doped by group IV elements, such as carbon (C), silicon (Si), and germanium (Ge) atom. The twelve hydrogen molecules (H2) were added to the outer surfaces of BNNT frameworks. Geometry optimization calculations were performed to find the local energy minima of the BNNTs nanostructures with the molecular hydrogens at the DFT/B3LYP/6-31G level of theory. By employing single-point calculations at the B3LYP/6-31G* level of theory, the equilibrium geometric structures were then utilized to find the electronic structures of hydrogen molecules adsorbed on the surfaces of BNNT frameworks. The results showed that the bond lengths of B-N are in the range of1.44 Å – 1.48 Å. The optimized distances of hydrogen molecules from the surfaces of BNNTs were predicted to be 3.1 Å – 3.2 Å. Moreover, the computed HOMO-LUMO energies of molecular hydrogens adsorbed on the surface of BNNTs are about 2.2 eV – 4.3 eV. For the surface map of HOMO, the electron density distribution of hydrogen molecules adsorbed on the surface of pristine BNNT was localized in the N-tip. While in the case of doped BNNTs, the electron densities of HOMOs were focused on the group IV elements. The B-tips on the pristine and doped BNNTs possess the major contribution to the LUMO. For the spin density distributions, the major spin densities of doped BNNTs were localized on the group IV elements.

Keywords: Density functional theory, hydrogen storage system, boron nitride nanotubes, electronic structures, HOMO-LUMO energies

Abstrak

Dalam laporan ini, teori fungsi ketumpatan (DFT) yang digunakan untuk menyiasat struktur dan sifat elektronik bagi hidrogen molekul yang terjerap ke atas permukaan tiub nano boron nitrida boron (BNNT) dengan/tanpa didop oleh unsur kumpulan IV, seperti atom karbon (C), silikon (Si), dan germanium (Ge). Selain itu, dua belas molekul hidrogen (H2) ditambahkan ke atas permukaan rangka kerja BNNT. Pengiraan pengoptimuman geometri yang dilakukan untuk mencari minima tenaga tempatan bagi struktur nano BNNT dengan hidrogen molekul pada tahap teori DFT/B3LYP/6-31G. Dengan menggunakan pengiraan titik tunggal pada tahap teori B3LYP/6-31G*, struktur geometri keseimbangan rangka kerja yang digunakan untuk mencari struktur elektronik bagi hidrogen molekul yang terjerap ke atas permukaan rangka kerja BNNT dalam kajian ini. Keputusan yang dikira menunjukkan bahawa panjang ikatan B-N yang diperoleh adalah kira-kira dalam julat 1.44 Å – 1.48 Å. Jarak optimum molekul hidrogen dari permukaan BNNTs ialah 3.1 Å - 3.2 Å. Selain itu, tenaga HOMO-LUMO yang dikira bagi hidrogen molekul yang terjerap ke atas permukaan BNNT adalah kira-kira 2.2 eV – 4.3 eV. Bagi plot HOMO, taburan ketumpatan elektron dalam BNNT yang tulen telah disetempatkan di hujung N, manakala ketumpatan elektron HOMO di BNNT yang didop adalah tertumpu pada unsur kumpulan IV. Untuk plot LUMO, semua keputusan yang dikira adalah sama, iaitu hujung B bagi semua BNNT mempunyai sumbangan yang paling besar. Dalam kes taburan ketumpatan putaran, ketumpatan putaran utama bagi kes BNNT yang didop telah disetempatkan pada elemen kumpulan IV.

Kata kunci: Teori fungsi ketumpatan, sistem penyimpanan hidrogen, tiub nano boron nitrida, struktur elektronik, tenaga HOMO-LUMO

1.0 INTRODUCTION

Boron nitride nanomaterials have attracted considerable attention with the developments of nanoscience and nanotechnology nowadays. For example, Joy *et al.*, in 2020 reviewed the nanostructure of boron nitride (BN) [1]. The BN is a crystalline compound, which consists of equal numbers of boron (B) and nitrogen (N) atoms. In the report, there have six crystalline forms of BNs, i.e. hexagonal, cubic, wurtzite, rhombohedral, amorphous, and turbostratic BNs. Among these BNs, the hexagonal form of boron nitride (h-BN) has attracted the highest attention recently due to the form of h-BN being similar to that of graphene. In addition, Angizi *et al.*, in 2022 also reviewed the fundamental properties (i.e. band structures and optoelectronic properties) of h-BN nanostructures and their applications due to h-BNs possessing excellent thermal and chemical stability in the literature studies [2].

To realize the progress of nanoscience and nanotechnology, many experimental and theoretical studies of hexagonal boron nitride (h-BN) nanomaterials have been undertaken in recent years. For example, Zhao *et al.*, in 2011 studied the adsorption of benzene molecule on the outer surface of a zigzag single-walled boron nitride nanotube (BNNT) at the ωB97X-D/6-31G** level of theory [3]. The computed nearest distance between the benzene ring and BNNT is about 3.07 A in the density functional theory (DFT) calculation. Moreover, the highest occupied molecular orbital (HOMO) and lowest unoccupied molecular orbital (LUMO) surface plots of benzene-modified BNNT were mainly localized on the BNNT framework, respectively. In the same year, Ju *et al.* investigated the electronic structures of (8, 0) zigzag and (5, 5) armchair models of BNNTs [4]. The findings noted that the B-N bond distances of armchair BNNT are about 1.454 Å – 1.460 Å, whereas the B-N bond lengths of zigzag BNNT were examined to be about 1.455 Å – 1.457 Å in the report. These bond distances of B-N obtained are close to those of literature studies. In 2014, Seyed-Talebi and Neek-Amal reported hexagonal boron nitride ($B_{48}N_{48}$) nanosheet terminated with 25 hydrogen (H) atoms [5]. The optimized B-N distances obtained are 1.420 Å – 1.447 Å at the B3LYP/6-31G*, X3LYP/6-31G*, and M06/6-31G* levels of theories. The HOMO-LUMO energy values were calculated to be 6.38 eV – 6.82 eV in the report. In the case of Frontier molecular orbital (FMO) diagrams, the computed findings showed that both electronic densities of HOMO and LUMO were localized at the N- and B-edges of the h-BN nanostructure. Moreover, by employing the scheme of Mulliken population analysis (MPA), the DFT charge distribution results presented that all boron atoms hold the positive charges, and the negative charges fall on the nitrogen atoms. While there have two different types of charge values (positive and negative charges) for the hydrogen (H) atoms used in the h-BN framework. In the same year, Chua Abdullah *et al.* studied the presence of h-BN and alumina (Al_2O_3) nanoparticles in engine oil [6]. In the case of h-BN nanoparticle additives in the engine oil, the results found that the wear rate and coefficient of friction for the ball are slightly lower than those of h-BN with and without Al_2O_3. Javan *et al.*, in 2017 studied the Soman and Chlorosoman adsorbed on the external surface of BNNTs [7]. In the study, the bond lengths of B-N were calculated to be 1.447 Å – 1.449 Å at the B3LYP/6-311G** and M06-2X/6-311G** levels of calculations. The computed DFT findings noted that most electron densities of the HOMO and LUMO have occurred at the N- and B-tips of BNNTs with Soman and Chlorosoman molecules. Furthermore, the molecular electrostatic potential (MEP) surface maps noted that the positive electrostatic potentials fall in the regions of N-tips. The B-tips of studied BNNT frameworks showed the negative electrostatic potentials in the work. In 2022, Guo *et al.* studied the flexoelectric effect in h-BN nanosheet using the first principle DFT investigation [8]. The findings showed that the flexoelectric coefficient of h-BN is higher than that of graphene in the work. To enhance the flexoelectricity of h-BNs, the configurations of B and N atoms were arranged into two coaxially curved surfaces. Moreover, the results found that the flexoelectric coefficient of h-BN can increase the band gap of double-walled BNNT in the work.

In this respect, BN nanomaterials have been proven to be promising materials in the applications of energy storage, electronic, optoelectronic, biomedical, and others. For example, Anota *et al.*, in 2013 investigated the interaction between oxygen (O) atoms and h-BN monolayers [9]. There have six studied configurations, such as O atom bonded to two N atoms, O atom bonded to two B atoms, O atom added on the top of N atom, O atom added on the top of B atom, O atom bonded to B-N dimer, and O atom added within the hexagonal. The BN nanosheet, in which the O bonded to the B-N dimer possesses the lowest local energy minima among all six studied configurations of BN frameworks. All computed bond distances of B-N are determined to be 1.43 A - 1.45 A. Due to the dipole moments of studied BN configurations being 0.0134 debye - 15.8400 debye, the finding of high polarity obtained in the work shows the good potential used in semiconductors. In 2018, Merlo *et al.* studied the biocompatibility properties of BN nanomaterials in the application of the medical field [10]. In 2020, Bilal *et al.* discussed the optoelectronic properties of h-BN, which can be used in electronic and optoelectronic applications [11]. In 2021, Shah-Naqvi *et al.* investigated the adsorption of hydrogen molecules on pure and doped BN monolayers [12]. The DFT calculation results show that the distances between hydrogen molecules and nitrogen atoms in the middle of BN nanosheets are about 3.2 Å – 3.3 Å. While the hydrogen molecules at the B- and N-edges are predicted to be about 2.9 Å – 3.0 Å in the investigation. Kamali *et al.*, in 2022 investigated the adsorption of metformin (MF) on the BN (i.e. $B_{24}N_{24}$), aluminum nitride (i.e. $Al_{24}N_{24}$), and other frameworks using density functional theory at B3PW91/6-311G** level of theory [13]. Among all studied cases, the results found that the HOMO-LUMO energy of the $B_{24}N_{24}$ cluster can only be increased by doping with other elements, i.e. aluminum and phosphorus atoms in the study. Therefore, this $B_{24}N_{24}$ framework could be used as a drug delivery system in the future.

In the development of hydrogen energy, the BN nano-structural materials have been considered a promising candidate material for hydrogen storage. In recent years, numerous hydrogen energy storage research works have been carried out. For example, Baierle *et al.*, in 2006 reported the adsorptions of atomic and molecular hydrogens on C-doped BNNTs using DFT calculations [14]. The binding energies of atomic and molecular hydrogens adsorbed on the C-doped BNNTs showed significantly changed from those of pure BNNTs. When the hydrogen atom adsorbed on the top of nitrogen atom, the weak binding energy (0.009 eV) was obtained in the work. Moreover, the electron densities of HOMO were localized on the C_N and C_B atoms of doped BNNT frameworks in the report. In 2011, Krishnan, *et al.* studied the hydrogen molecules adsorbed on the zigzag graphene and h-BN monolayers [15]. The edges of the studied frameworks were terminated with hydrogen atoms in the report. There have several positions of molecular hydrogens on the studied nanosheets. For h-BN nanostructures, the hydrogen molecules were placed on the top of the B atom, top of the N atom, hallow, and bridge in the work. The computed binding energies obtained are about from -0.04 eV to -0.01 eV. In addition, the hydrogen molecules adsorbed on the external surfaces of zigzag BNNTs and carbon nanotubes (CNTs) were also carried out in the report. In the case of BNNT frameworks, the binding energies obtained in the report are close to those of BN sheets. These binding energies obtained from DFT calculations are still well below the desired experimental values. In 2006, Wu *et al.* studied the adsorption of molecular hydrogens on the external surfaces of platinum-doped BNNT frameworks using the DFT method [16]. In the study, the calculation results presented that the binding energy of hydrogen molecule in the doped BNNT is smaller than that of pristine BNNT. Moreover, the decrease of the hydrogen molecule adsorption energy in the Pt-doped BNNT was obtained by increasing the number of H_2 molecule from one to two in the study. In the same year, Cabria *et al.* reported the adsorption of hydrogen molecule (H_2) on the outer surface of carbon nanotube (CNT) using a DFT technique [17]. The computed DFT results noted that the binding energy (BE) obtained is about 0.1 eV/H_2 molecule in the report. Moreover, the distances between two neighbor hydrogen molecules are about 2.5 Å - 4.1 Å, due to the H_2-H_2 showing strong intermolecular repulsion when the distance between two hydrogen molecules is less than 2.5 A. The results obtained are consistent with the finding presented by Diep and Jahson in 2000 [18]. Diep and Jahson reported the lowest potential energy minimum range for two neighbor molecular hydrogens were placed at the separation distances of 2.7 Å - 4.5 Å. In 2021, Sunnardianto *et al.* studied the H_2 molecule adsorption and desorption on the hydrogenated defective graphene nanosheet [19]. The computed results noted that the hydrogenated defective graphene nanostructure possesses a better hydrogen molecule storage environment as compared to that of pristine graphene in the work.

Recently, BNNT among BN nanostructures materials has attracted a lot of research attention due to its possessing a similar tubular nanostructure to carbon nanotube (CNT). For example, Ghosh *et al.*, in 2010 reported the electronic and magnetic properties of the transition metals adsorbed on the inner and outer surfaces of BNNTs [20]. Regardless of the diameter size of the nanotube, the magnetic characteristics of all studied BNNTs are almost the same in the investigation. In the same year, Mirzaei and his co-worker also presented the BNNT frameworks using DFT/B3LYP/6-31G* level of theory

[21, 22]. The structures of BNNT (6,0) were terminated with oxygen and sulfur atoms in the work, respectively. The DFT calculations found that the B-N bond lengths obtained from the BNNT with oxygen and oxygen and sulfur termination are the same with that of hydrogen termination. In 2012, Moradi *et al.* used DFT method to determine the electronic properties (i.e. binding energies, Frontier molecular orbitals, and others) of thiazole molecule adsorbed on the outer surface of BNNT (6,0) framework [23]. The computational results noted that the HOMO-LUMO energy of thiazole molecule adsorbed on the BNNT model is smaller than that of pure BNNT. This is because of a decrease in the stability with an increase of thiazole molecule adsorbed on the BNNT framework. In 2015, Kaur *et al.* studied the adsorption of drugs (i.e. oxazole and isoxazole) on the surfaces of zigzag BNNT (6,0) and armchair BNNT (5,5), respectively [24]. The results noted the structural changes in the adsorption site of BNNT (6,0), while for armchair BNNT, there is no change in the adsorption site. In 2020, Sotudeh *et al.* studied the optical properties and electronic structures of BNNT (6,0) using DFT technique [25]. The results found that the optical parameters (i.e. dielectric constants, energy loss function, optical conductivity constant, and others) are in good agreement with the experiment. In addition, they also mentioned that the energy band gap of BNNT does not depend on the diameter and chirality of the tube. Motivated by the recent experimental/theoretical progress in hydrogen storage, and the balance between the computational cost/accuracy considerations, we have employed the first-principles DFT method to investigate the interaction of molecular hydrogens with the pristine and group IV doped BNNTs. Since most the previous literature studies have focused on the (6,0) single-walled BNNT, the structural and electronic properties of hydrogen molecules adsorbed on the outer surface of pure and doped (6,0) BNNTs are determined in this work. The details of the computational methodology, results, discussion, and conclusion are reported in the following sections.

2.0 METHODOLOGY

To investigate the effect of molecular hydrogen absorbed on the outer surface of pristine and C/Si/Ge-doped BNNTs, the method of DFT was conducted to find the geometric and electronic structures of hydrogen molecules adsorbed on BNNT (6,0) frameworks (i.e. $B_{36}N_{36}H_{12}\cdot12H_2$, $B_{35}CN_{36}H_{12}\cdot12H_2$, $B_{36}N_{35}CH_{12}\cdot12H_2$, $B_{35}SiN_{36}H_{12}\cdot12H_2$, $B_{36}N_{35}SiH_{12}\cdot12H_2$, $B_{35}GeN_{36}H_{12}\cdot12H_2$, and $B_{36}N_{35}GeH_{12}\cdot12H_2$). In this study, both N- and B-tips of pure and doped BNNT frameworks were terminated with twelve hydrogen atoms in this study, which was reported by Krishnan, *et al.* (in 2011) and Xiang *et al.* (in 2019) [15, 26]. All DFT calculations were performed using Gaussian 09 program package [27].

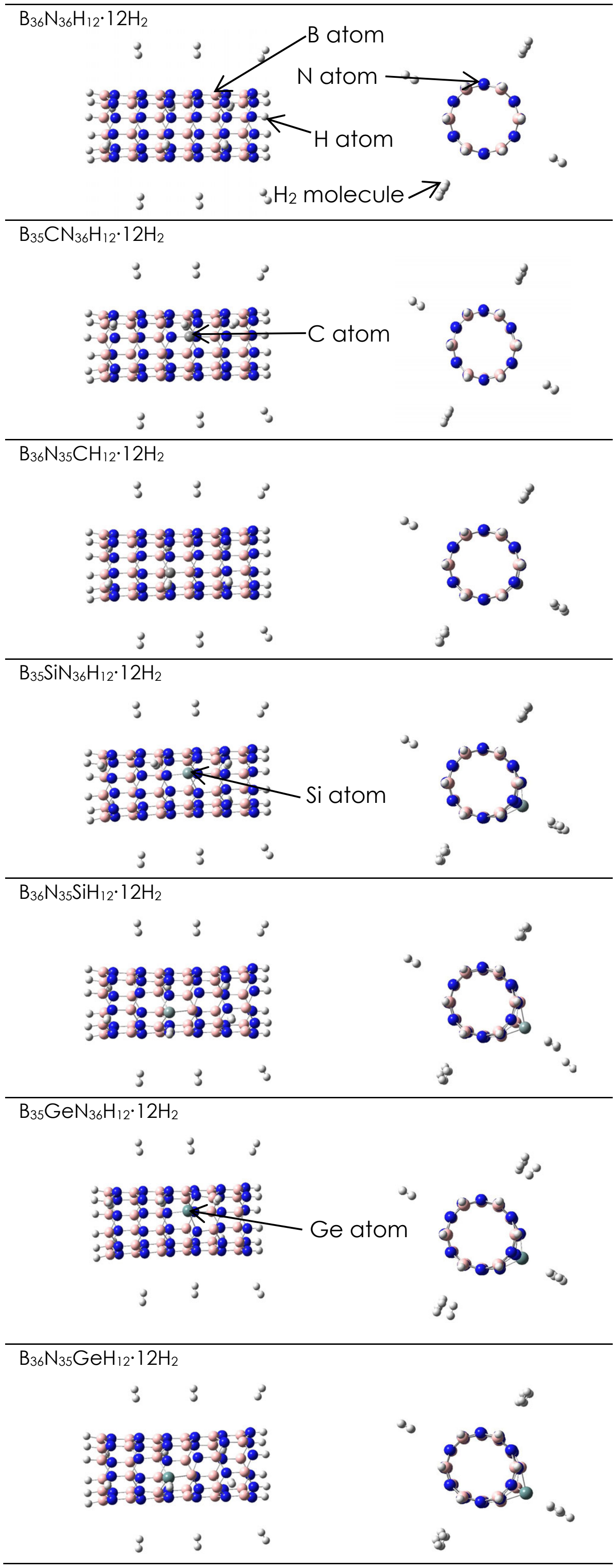

Figure 1 Optimized geometric structures of molecular hydrogens absorbed on the external surfaces of pristine and group IV doped BNNTs, where N (blue ball), B (pink ball), H (white ball), C (grey ball), Si (blue-grey ball), and Ge (green-grey ball)

At the B3LYP/6-31G level of theory, geometry optimization calculations were performed to find the equilibrium structures of twelve hydrogen molecules absorbed on the external surfaces of pure and doped BNNTs. Figure 1 illustrates the optimized hydrogen molecules adsorbed on the surface of pristine and doped BNNTs. By employing single-point calculations, the optimized geometric structures of title frameworks were then used to determine the electronic structures (i.e. binding energies, Frontier molecular orbitals, and others) of hydrogen molecules adsorbed on the external surfaces of pure and group IV doped BNNTs at the B3LYP/6-31+G* level of theory.

3.0 RESULTS AND DISCUSSION

To understand the fundamental interactions between molecular hydrogens and BNNTs, our DFT calculation results note that the optimized B-N bond lengths are examined to be in the range of 4.4 Å – 4.7 Å in this study. These bond distances are consistent with those of literature studies reported by Ju *et al.* (in 2011), Seyed-Talebi, and Neek-Amal (in 2014) [4, 5]. Moreover, the hydrogen molecules placed on the outer surface of pure and doped BNNT frameworks are about 3.1 Å – 3.2 Å.

These computed distances obtained in this study are slightly shorter than those of BN nanosheets (3.2 Å – 3.3 Å) presented by Shah-Naqvi *et al.* in 2021 [12]. In Table 1, the computed binding energies of hydrogen molecules adsorbed on pristine and group IV doped BNNTs are about 0.005 eV – 0.008 eV per molecular hydrogen. The results found that the binding energies of molecular hydrogen adsorbed on group IV doped BNNTs are slightly increased than that of pure BNNT. Moreover, the binding energies increase from carbon to silicon, and then to germanium. Overall, these binding energy values obtained in this work are still smaller than those of literature values [9, 11, 16]. In the table, the values of BSSE energies are determined to be from 0.187 eV to 0.240 eV. The computed dipole moments do not show many significant changes for pure and doped BNNTs.

In this study, the corresponding dipole moments fall in the range of 5.172 Debye – 5.6499 Debye. In addition, the HOMO-LUMO energies of hydrogen molecules adsorbed on pure and doped BNNTs are also reported in Table 1. The computed results note that the corresponding HOMO-LUMO energies are in the range of 2.166 eV - 4.312 eV. When one of the B atoms is substituted by group IV elements (i.e. carbon, silicon, and germanium atoms) in the studied BNNT frameworks, the HOMO-LUMO energies obtained from DFT calculations are increased from carbon to germanium (2.166 eV, 3.903 eV, and 4.052 eV). The opposite results are found when one of the N atoms is substituted by group IV elements. The HOMO-LUMO energy values are decreased from carbon to germanium (4.198 eV, 3.939 eV, and 3.760 eV) in this study. However, the HOMO-LUMO energies of doped BNNTs showed significant changes with that of pristine BNNT obtained in the study. The surface diagrams of Frontier molecular orbitals (FMOs) of studied BNNTs are illustrated in Figure 2. For the pure BNNT, the electron density distribution of HOMO is focused in the region of the N-tip, whereas the B-tip holds the major electron densities in LUMO of pristine BNNT. In the case of doped BNNT frameworks, the electron densities of HOMOs are mainly localized in the region around the group IV elements, such as C, Si, or Ge atoms. While the electron density distributions of LUMOs are contributed from p_z-orbitals at B-tips, which is close to that of pure BNNT in this work. In addition, these Frontier molecular orbital results are also close to those of BN nanostructures in the literature studies [3, 5, 7, 15].

Table 1 Computed binding energies (eV), BSSE energies (eV), Frontier molecular orbital energies (eV), and dipole moments (debye) of hydrogen molecules adsorbed on the outer surfaces of pristine and doped BNNTs

	$B_{36}N_{36}H_{12}\cdot 12H_2$	**$B_{35}CN_{36}H_{12}\cdot 12H_2$**
Binding energy	0.0048	0.0046
BSSE energy	0.1925	0.1919
HOMO	-6.6034	-4.4205
LUMO	-2.2912	-2.2545
HOMO-LUMO Energy	4.3122	2.1660
Dipole moment	5.2405	5.1719
	$B_{36}N_{35}CH_{12}\cdot 12H_2$	**$B_{35}SiN_{36}H_{12}\cdot 12H_2$**
Binding energy	0.0050	0.0053
BSSE energy	0.1905	0.1937
HOMO	-6.4638	-6.1430
LUMO	-2.2662	-2.2403
HOMO-LUMO Energy	4.1976	3.9027
Dipole moment	5.4651	5.4797
	$B_{36}N_{35}SiH_{12}\cdot 12H_2$	**$B_{35}GeN_{36}H_{12}\cdot 12H_2$**
Binding energy	0.0049	0.0069
BSSE energy	0.1866	0.2401
HOMO	-6.2203	-6.2736
LUMO	-2.2811	-2.2221
HOMO-LUMO Energy	3.9391	4.0515
Dipole moment	5.5874	5.6499
	$B_{36}N_{35}GeH_{12}\cdot 12H_2$	
Binding energy	0.0078	
BSSE energy	0.2403	
HOMO	-6.0436	
LUMO	-2.2841	
HOMO-LUMO Energy	3.7595	
Dipole moment	5.6181	

$B_{36}N_{36}H_{12}\cdot 12H_2$

HOMO

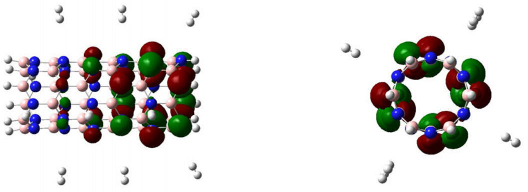

LUMO

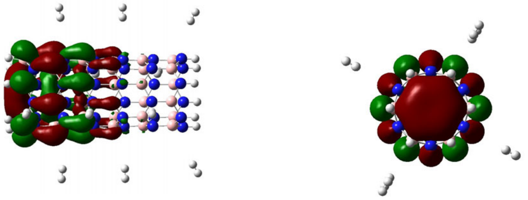

$B_{35}CN_{36}H_{12}\cdot 12H_2$

HOMO

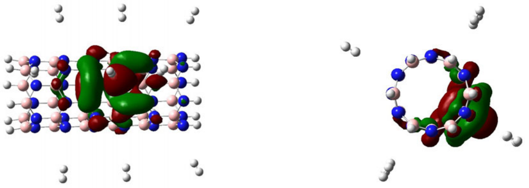

LUMO

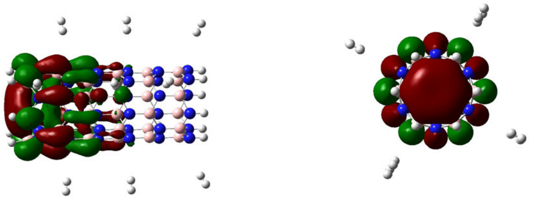

$B_{36}N_{35}CH_{12}\cdot 12H_2$

HOMO

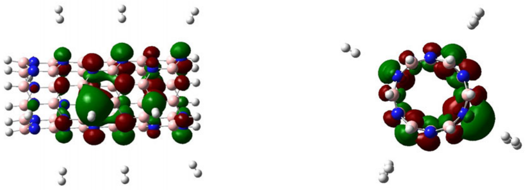

LUMO

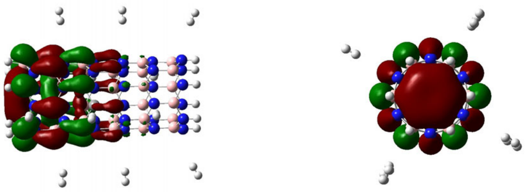

$B_{35}SiN_{36}H_{12}\cdot 12H_2$

HOMO

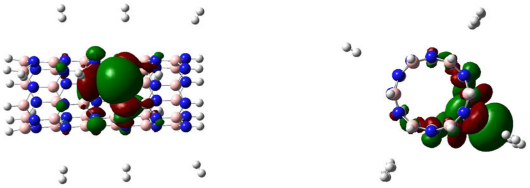

LUMO

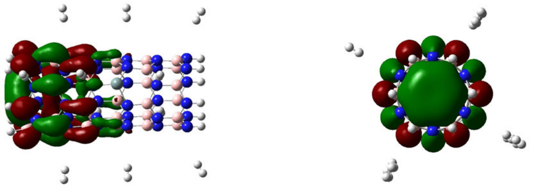

$B_{36}N_{35}SiH_{12}\cdot 12H_2$

HOMO

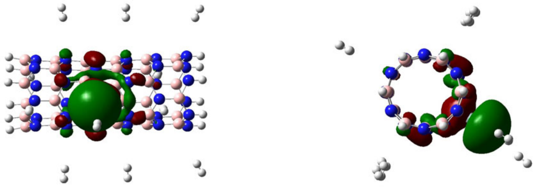

LUMO

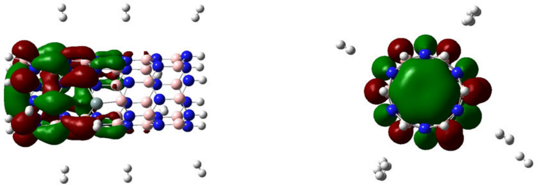

$B_{35}GeN_{36}H_{12}\cdot 12H_2$

HOMO

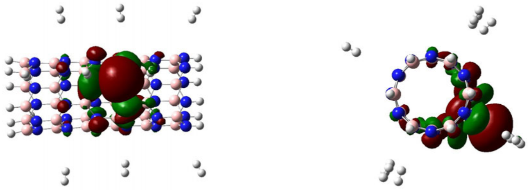

LUMO

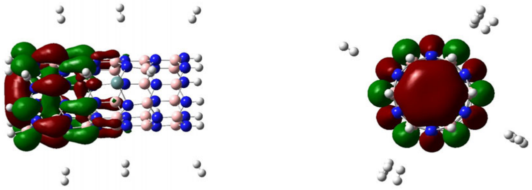

$B_{36}N_{35}GeH_{12}\cdot 12H_2$

HOMO

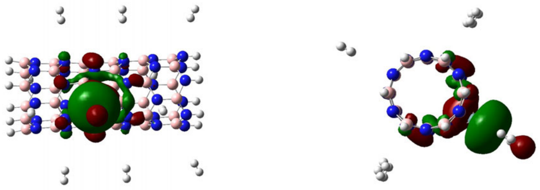

LUMO

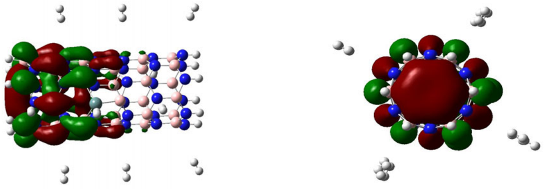

Figure 2 Surface plots of Frontier molecular orbitals of molecular hydrogens adsorbed on the surfaces of pure and doped BNNTs

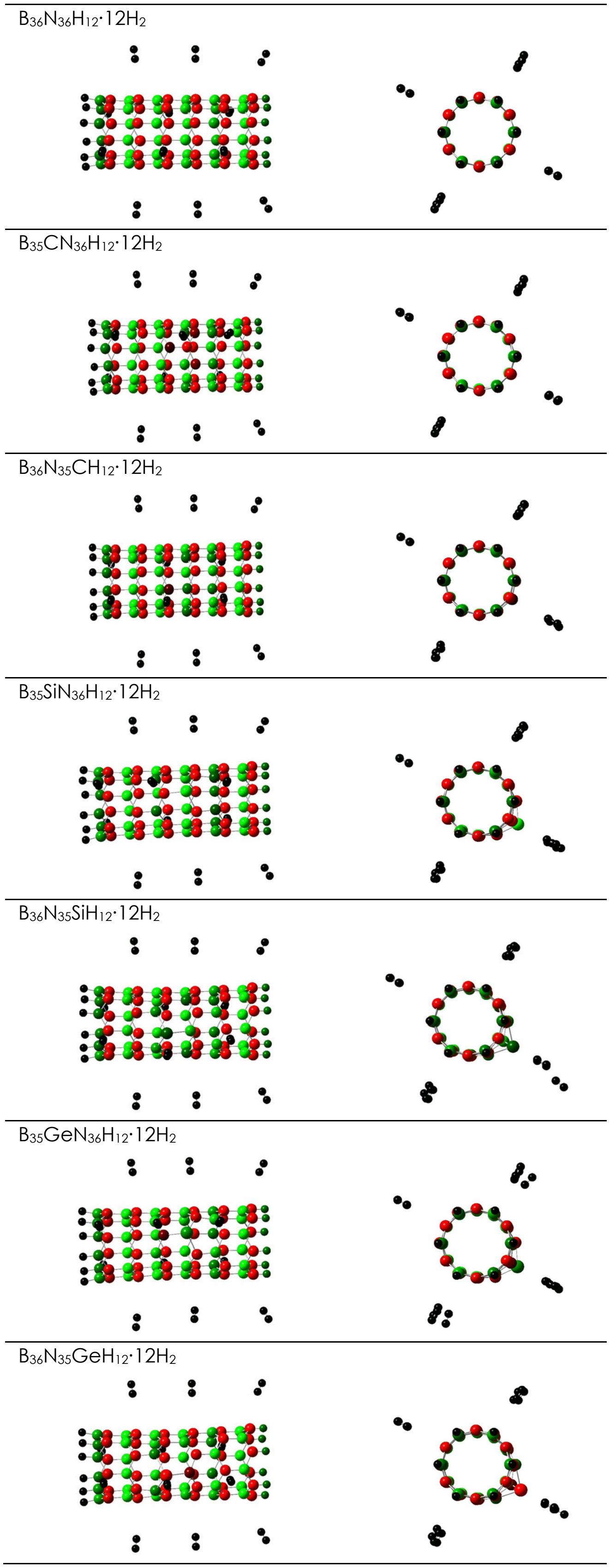

$B_{36}N_{36}H_{12}\cdot 12H_2$

$B_{35}CN_{36}H_{12}\cdot 12H_2$

$B_{36}N_{35}CH_{12}\cdot 12H_2$

$B_{35}SiN_{36}H_{12}\cdot 12H_2$

$B_{36}N_{35}SiH_{12}\cdot 12H_2$

$B_{35}GeN_{36}H_{12}\cdot 12H_2$

$B_{36}N_{35}GeH_{12}\cdot 12H_2$

Figure 3 Computed Mulliken atomic charges of hydrogen molecules adsorbed on the outer surfaces of pure and doped BNNTs

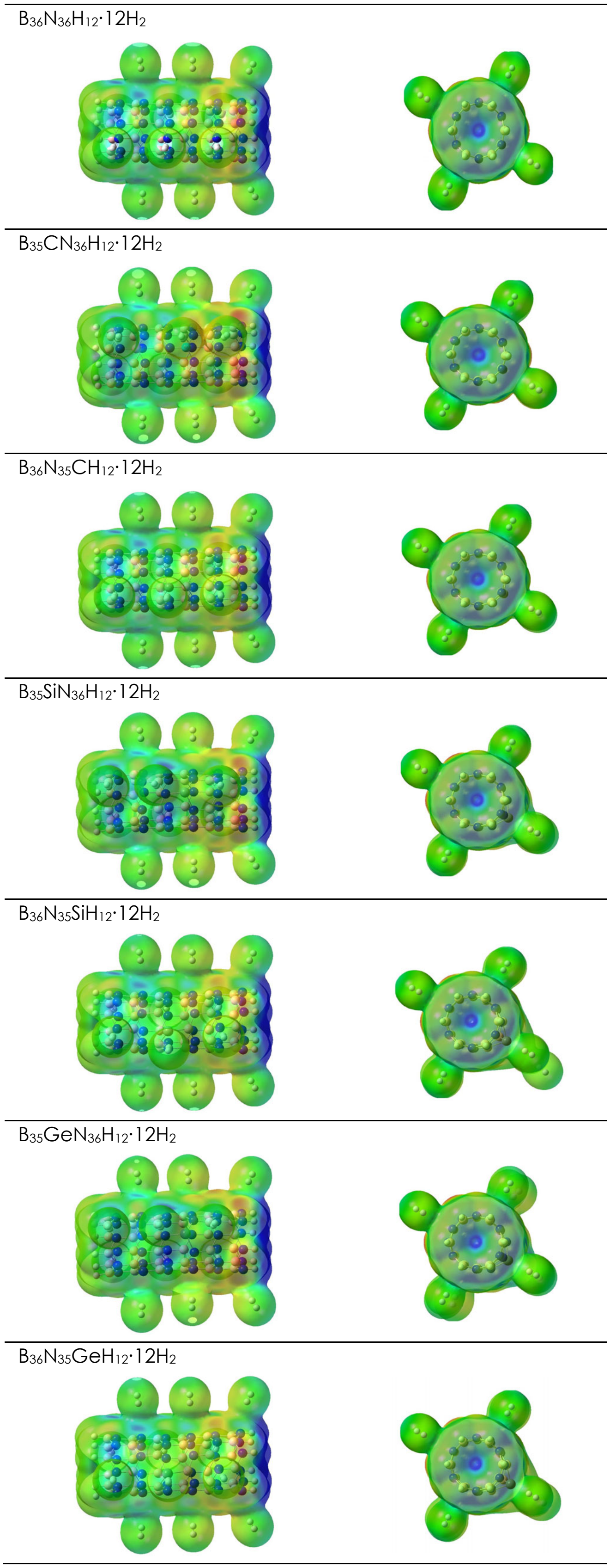

$B_{36}N_{36}H_{12}\cdot 12H_2$

$B_{35}CN_{36}H_{12}\cdot 12H_2$

$B_{36}N_{35}CH_{12}\cdot 12H_2$

$B_{35}SiN_{36}H_{12}\cdot 12H_2$

$B_{36}N_{35}SiH_{12}\cdot 12H_2$

$B_{35}GeN_{36}H_{12}\cdot 12H_2$

$B_{36}N_{35}GeH_{12}\cdot 12H_2$

Figure 4 Optimized molecular electrostatic potentials of hydrogen molecules adsorbed on the outer surfaces of pure and doped BNNTs

Using the scheme of Mulliken atomic population (MAP), Figure 3 shows the electronic atomic charge distributions of molecular hydrogens adsorbed on the external surfaces of pristine and doped BNNT frameworks. The computed DFT results note that all B atoms show positive charges (0.321 *a.u.* – 1.638 *a.u.*), and the negative charges (between -1.233 *a.u.* and -0.479 *a.u.*) are localized on the N atoms. Moreover, the group IV elements (i.e. C, Si, and Ge atoms) have positive and negative charges in the investigation. For example, when one of the B atoms localized in the middle of BNNTs is substituted by C, Si, or Ge atom, the charges of group IV elements are obtained, with the corresponding charges of -1.070 *a.u.* – 2.695 *a.u.* in this report. When one of the N atoms located in the middle of BNNTs is substituted by C, Si, or Ge atom, the charge values of group IV elements are predicted to be between -1.051 *a.u.* and -0.319 *a.u.* in this study. In addition, the calculated findings also note that the positive charge values of B atoms located in N-tips are slightly higher than those of B-tips in all studied BNNT frameworks. While the negative charge values of N atoms focused on B-tips are slightly smaller than those of N-tips due to the strong bonds between the N and H-terminating atoms are found in this work. These Mulliken atomic charges (MACs) obtained are consistent with those of results reported by Seyed-Talebi and Neek-Amal in 2014 [5]. In addition, the surface plots of molecular electrostatic potentials (MEPs) are also illustrated in Figure 4. The results of MEPs obtained are similar to those of MACs. The color code of MEP surface plot used in this work is between -2.5×10^{-2} (red) to 2.5×10^{-2} (blue). The blue color surface maps in these diagrams represent the positive electrostatic potentials in the studied BNNT frameworks, whereas the negative electrostatic potentials possess yellow/red color surface plots. The N-tips of studied BNNT frameworks are surrounded by the greater positive electrostatic potentials. While the regions near B-tips possess the negative electrostatic potentials in this study. The results of MEPs reported are in good agreement with the findings presented by Javan *et al.* in 2017 [7].

The computed spin density distributions of hydrogen molecules adsorbed on the outer surfaces of group IV doped BNNTs are presented in Figure 5. The blue color surfaces in the diagrams represent the positive spin densities in the studied frameworks, whereas the negative spin density distribution is presented using green color surface plots. The DFT results note that the spin density distributions are concentrated mostly in the group IV elements, such as C, Si, and Ge atoms in the studied BNNT frameworks. The corresponding calculated spin density values of C, Si, and Ge atoms are found to be about 0.725 – 1.090 in this report. In addition, the computed findings also report that when one of the B atoms is substituted by group IV elements in the studied BNNT frameworks, the spin density values (0.725 – 1.014) of C, Si, and Ge atoms are calculated to be slightly smaller than those of nitrogen atoms substituted by group IV elements in the BNNTs (0.801 – 1.090). This is because some spin density distributions are transferred to N atoms of the studied BNNT systems to adsorb the molecular hydrogens in this work. Moreover, the computed spin densities of hydrogen molecules in the studied BNNT nanostructures are predicted to be very small.

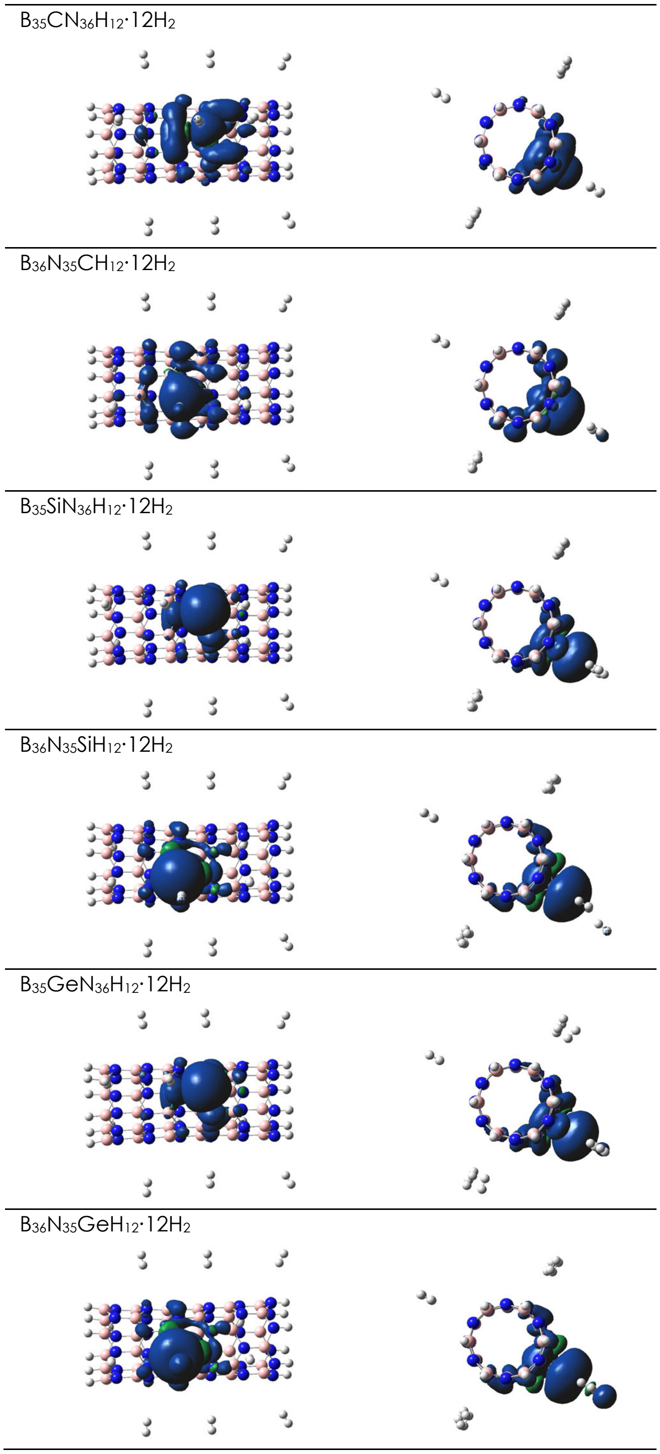
$B_{35}CN_{36}H_{12}\cdot 12H_2$

$B_{36}N_{35}CH_{12}\cdot 12H_2$

$B_{35}SiN_{36}H_{12}\cdot 12H_2$

$B_{36}N_{35}SiH_{12}\cdot 12H_2$

$B_{35}GeN_{36}H_{12}\cdot 12H_2$

$B_{36}N_{35}GeH_{12}\cdot 12H_2$

Figure 5 Calculated spin densities of molecular hydrogens absorbed on the external surfaces of group IV doped BNNTs

4.0 CONCLUSION

Using DFT method, the adsorption of hydrogen molecules on the outer surfaces of pristine and group IV doped BNNTs were investigated. In this study, twelve hydrogen molecules can be adsorbed on the outer surface of the tubes. The DFT calculations found the weak hydrogen molecule binding energies obtained in this work. The HOMO-LUMO energies are about 2.2 eV – 4.3 eV, which are close to those of literature studies. Using the scheme of MAP, all B and N atoms showed positive and negative charges, respectively. The group IV elements (i.e. C, Si, and Ge atoms) possess the positive and negative charge values in this study. For the surface maps of MEPs, the computed results are consistent with those of MACs. In this report, the B-tips of BNNTs hold the negative electrostatic potentials, while the highest positive electrostatic potentials fall in the region of N-tips. Therefore, our computation study takes insight on the electronic properties of pristine and doped BNNTs as function of hydrogen molecular.

Acknowledgement

The research was supported by the Ministry of Higher Education (MoHE), through the Fundamental Research Grant Scheme FRGS/1/2018/TK10/UTAR/02/7.

References

[1] Joy, J., George, E., Haritha, P., Thomas, S. & Anas, S. 2020. An Overview of Boron Nitride based Polymer Nanocomposites. *Journal of Polymer Science*. 58: 3115-3141. DOI: 10.1002/pol.20200507.

[2] Angizi, S., Alem, S. A. A. & Pakdel, A. 2022. Towards Integration of Two-Dimensional Hexagonal Boron Nitride (2D h-BN) in Energy Conversion and Storage Devices. *Energies*. 15(3): 1162(1-34). DOI: 10.3390/en15031162.

[3] Zhao, Y., Wu, X., Yang, J. & Zeng, X. C. 2011. Ab Initio Theoretical Study of Non-covalent Adsorption of Aromatic Molecules on Boron Nitride Nanotubes. *Physical Chemistry Chemical Physics*. 12(24): 11766-11772. DOI: 10.1039/c1cp20534j.

[4] Ju, S. P., Wang Y. C. & Lien T. W. 2011. Tuning the Electronic Properties of Boron Nitride Nanotube by Mechanical Uni-axial Deformation: A DFT Study. *Nanoscale Research Letters*. 6(1): 160(1-11). DOI: 10.1186/1556-276x-6-160.

[5] Seyed-Talebi, S. M. & Neek-Amal, M. 2014. The Different Adsorption Mechanism of Methane Molecule onto a Boron Nitride and a Graphene Flakes. *Journal of Applied Physics*. 116(15): 153507(1-7). DOI: 10.1063/1.4898336.

[6] Chua Abdullah, M. I. H., Abdollah, M. F., Amiruddin, H., Tamaldin, N. & Nuri, N. R. M. 2014. Effect of hBN/Al2O3 Nanoparticle Additives on the Tribological Performance of Engine Oil. *Jurnal Teknologi*. 66(3): 1-6. DOI: 10.11113/jt.v66.2685.

[7] Javan, M. B., Soltani, A., Ghasemi, A. S., Lemeski, E. T., Gholami, N. & Balakhenyli, H. 2017. Ga-doped and Antisite Double Defects Enhance the Sensitivity of Boron Nitride Nanotubes towards Soman and Chlorosoman. *Applied Surface Science*. 411: 1-10. DOI: 10.1016/j.apsusc.2017.03.187

[8] Guo, H., Yang, T., Xuan, X., Zhang, Z. & Guo, W. 2022. Flexoelectricity in Hexagonal Boron Nitride Monolayers. *Extreme Mechanics Letters*. 52: 101669(1-7). DOI: 10.1016/j.eml.2022.101669.

[9] Anota, E. C., Juárez, A. R., Castro, M. & Cocoletzi, H. H. 2013. A Density Functional Theory Analysis for the Adsorption of the Amine Group on Graphene and Boron Nitride Nanosheets. *Journal of Molecular Modelling*. 19(1): 321-328. DOI: 10.1007/s00894-012-1539-4.

[10] Merlo, A., Mokkapati, V. R. S. S., Pandit, S. & Mijakovic, I. 2018. Boron Nitride Nanomaterials: Biocompatibility and Bio-applications. *Biomaterials Science*. 6: 2298-2311. DOI: 10.1039/C8BM00516H.

[11] Bilal, M., Xu, W., Wang, C., Wen, H., Zhao, X., Song, D. & Ding, L. 2020. Optoelectronic Properties of Monolayer Hexagonal Boron Nitride on Different Substrates Measured by Terahertz Time-Domain Spectroscopy. *Nanomaterials (Basel)*. 10(4): 762(1-11). DOI: 10.3390/nano10040762.

[12] Shah Naqvi, S. A. A., Toh P. L., Wang. S. M., Lim, Y. C., Ang, L. S. & Sim L. C. 2021. Computational Study of Hydrogen Molecules Adsorption on Boron Nitride with/without Adopted by One of Elements from Group IV. *IOP Conference Series: Earth and Environmental Science*. 945: 012001(1-7). DOI: 10.1088/1755-1315/945/1/012001.

[13] Kamali, F., Ebrahimzadeh-Rajaei, G., Mohajeri, S., Shamel, A., & Khodadadi-Moghaddam, M. 2022. A Computational Design of X24Y24 (X= B, Al, and Y= N, P) Nanoclusters as Effective Drug Carriers for Metformin Anticancer Drug: A DFT Insight. *Inorganic Chemistry Communications*. 109527. DOI: 10.1016/j.inoche.2022.109527.

[14] Baierle, R. J., Piquini, P., Schmidt, T. M. & Fazzio, A. 2006. Hydrogen Adsorption on Carbon-Doped Boron Nitride Nanotube. *Journal of Physical Chemistry B*. 110(42): 21184-21188. DOI: 10.1021/jp061587s.

[15] Krishnan, S., Vadapoo, R., Riley, K. E. & Velev, J. P. 2011. Dispersion-corrected Density Functional Theory Comparison of Hydrogen Adsorption on Boron-nitride and Carbon Nanotubes. *Physical Review B*. 84: 165408(1-6). DOI:10.1103/PhysRevB.84.165408.

[16] Wu, X., Yang, J. L. & Zeng, X. C. 2006. Adsorption of Hydrogen Molecules on the Platinum-doped Boron Nitride Nanotubes. *Journal of Chemical Physics*. 125: 044704(1-6). DOI: 10.1063/1.2210933.

[17] Cabria, I., López, M.J. & Alonso, J. A. 2006. Density Functional Study of Molecular Hydrogen Coverage on Carbon Nanotubes. *Computational Materials Science*. 35(3): 238-242. DOI: 10.1016/j.commatsci.2004.10.008.

[18] Diep, P. & Johnson, J. K. 2000. An Accurate H2-H2 Interaction Potential from First Principles. Journal of Chemical Physics. *Journal of Chemical Physics*. 112(10): 4465-4473. DOI: 10.1063/1.481009.

[19] Sunnardianto, G. K., Bokas, G., HUssein. A., Walters, C., Moultos, O. A. & Dey, P. 2021. Efficient Hydrogen Storage in Defective Graphene and its Mechanical Stability: A Combined Density Functional Theory and Molecular Dynamics Simulation Study. *International Journal of Hydrogen Energy*. 46(7): 5485-5494. DOI: 10.1016/j.ijhydene.2020.11.068.

[20] Ghosh, S., Nigam, S., Das, G. P. & Majumdar, C. 2010. Novel Properties of Boron Nitride Nanotubes Encapsulated with Fe, Co, and Ni Nanoclusters. *Journal of Chemical Physics*. 132: 164704(1-8). DOI: 10.1063/1.3381183.

[21] Mirzaei, M. & Mirzaei, M. 2010. A Computational Study of Oxygen-termination of a (6,0) Boron Nitride Nanotube. *Monatshefte Für Chemie/Chemical Monthly*. 141: 491-494. DOI: 10.1007/S00706-010-0287-3.

[22] Mirzaei, M. & Mirzaei, M. 2010. Sulfur Doping at the Tips of (6,0) Boron Nitride Nanotube: A DFT Study. *Physica E*. 42: 2147-2150. DOI: 10.1016/J.PHYSE.2010.04.014.

[23] Moradi, A. V., Peyghan, A. A., Hashemian, S. & Baei, M. T. 2012. Theoretical Study of Thiazole Adsorption on the (6,0) Zigzag Single-Walled Boron Nitride Nanotube. *Bulletin of the Korean Chemical Society*. 33(10): 3285-3292.

DOI: 10.5012/bkcs.2012.33.10.3285.

[24] Kaur, J., Singala, P. & Goel N. 2015. Adsorption of Oxazole and Isoxazole on BNNT Surface: A DFT Study. *Applied Surface Science*. 328: 632-640. DOI: 10.1016/j.apsusc.2014.12.099.

[25] Sotudeh, M., Boochani, A., Parhizgar, S. S. & Masharian, S. R. 2020. Optical and Electronic Properties of Zigzag Boron Nitride Nanotube (6,0): DFT Study. *International Nano Letters*. 10: 293-301. DOI: 10.1007/s40089-020-00314-w.

[26] Xiang, C., Li, A., Yang, S., Lan, Z., Xie, W., Tang, Y., Xu, H., Wang, Z. & Gu. H. 2019. Enhanced Hydrogen Storage Performance of Graphene Nanoflakes Doped with Cr Atoms: A DFT Study. *RSC Advances*. 9: 25690-25696. DOI: 10.1039/c9ra04589a.

[27] Frisch, M. J., Trucks, G. W., Schlegel, H. B., Scuseria, G. E., Robb, M. A., Cheeseman, J.R., Scalmani, G., Barone, V., Petersson, G. A., Nakatsuji, H., Li, X., Caricato, M., Marenich, A. V., Bloino, J., Janesko, B. G., Gomperts, R., Mennucci, B., Hratchian, H. P., Ortiz, J.V., Izmaylov, A. F., Sonnenberg, J. L., Williams-Young, D., Ding, F., Lipparini, F., Egidi, F., Goings, J., Peng, B., Petrone, A., Henderson, T., Ranasinghe, D., Zakrzewski, V. G., Gao, J., Rega, N., Zheng, G., Liang, W., Hada, M., Ehara, M., Toyota, K., Fukuda, R., Hasegawa, J., Ishida, M., Nakajima, T., Honda, Y., Kitao, O., Nakai, H., Vreven, T., Throssell, K., Montgomery, J. A., Jr., Peralta, J. E., Ogliaro, F., Bearpark, M. J., Heyd, J. J., Brothers, E. N., Kudin, K. N., Staroverov, V. N., Keith, T. A., Kobayashi, R., Normand, J., Raghavachari, K., Rendell, A. P., Burant, J. C., Iyengar, S. S., Tomasi, J., Cossi, M., Millam, J. M., Klene, M., Adamo, C., Cammi, R., Ochterski, J. W., Martin, R. L., Morokuma, K., Farkas, O., Foresman, J. B. & Fox, D. J. 2016. *Gaussian 09*. Gaussian, Inc from Wallingford CT, USA.